Conductive Cobalt doped Niobium Nitride Porous Spheres as Efficient Polysulfide Convertor for Advanced Lithium-Sulfur Batteries

Weini Ge,[a] *Lu Wang*,[a] *Chuanchuan Li*,[a] *Chunsheng Wang*,[a] *Debao Wang*,[b] *Yitai Qian*[a] *and Liqiang Xu**[a, c]

[a] Key Laboratory of Colloid & Interface Chemistry (Shandong University), Ministry of Education and School of Chemistry and Chemical Engineering, Shandong University, Jinan 250100, P. R. China

[b]College of Chemistry and Molecular Engineering,Qingdao University of Science and Technology, Qingdao 266042, P. R. China

[c] Key Laboratory of Advanced Energy Materials Chemistry (Ministry of Education), Nankai University, Tianjin 300071, P. R. China

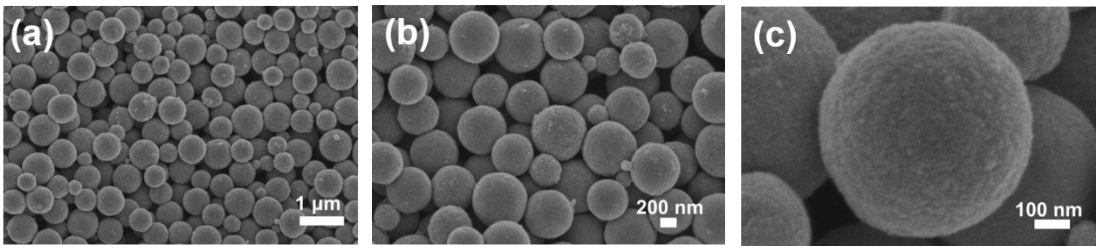

Fig. S1 FESEM images of the precursor of Co-NbN.

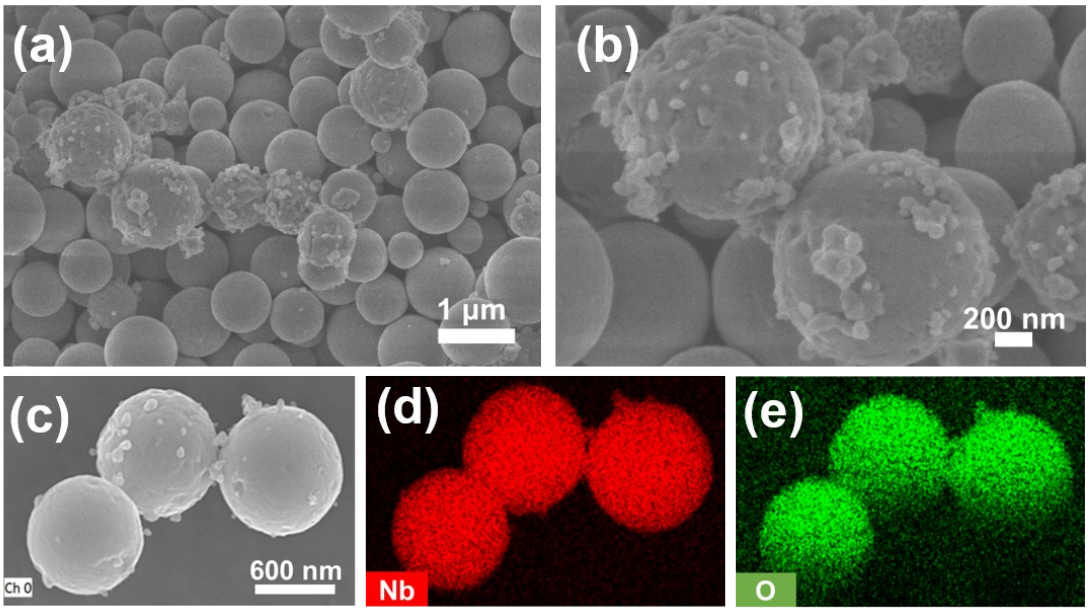

Fig. S2 (a, b) FESEM images of Nb_2O_5. (c-e) SEM images and the corresponding EDS elemental mapping.

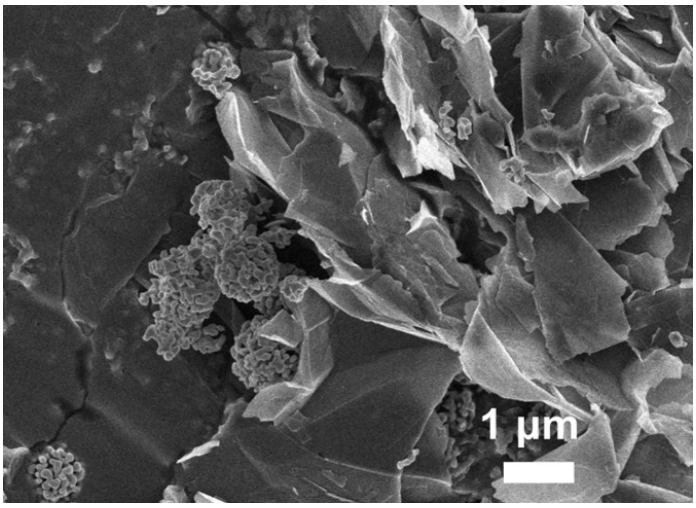

Fig. S3 The FESEM image of the obtained Co-NbN/rGO/S composite.

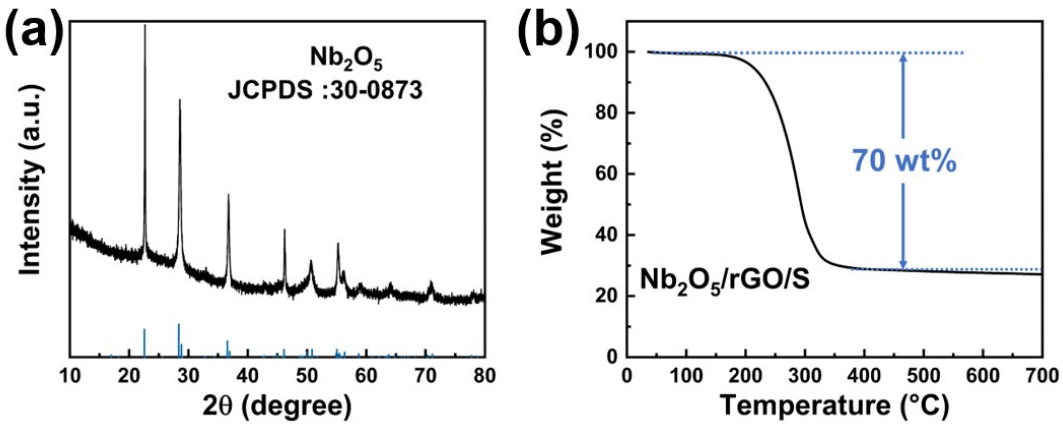

Fig. S4 (a) XRD pattern of Nb_2O_5. (b) TGA curve of Nb_2O_5/rGO/S.

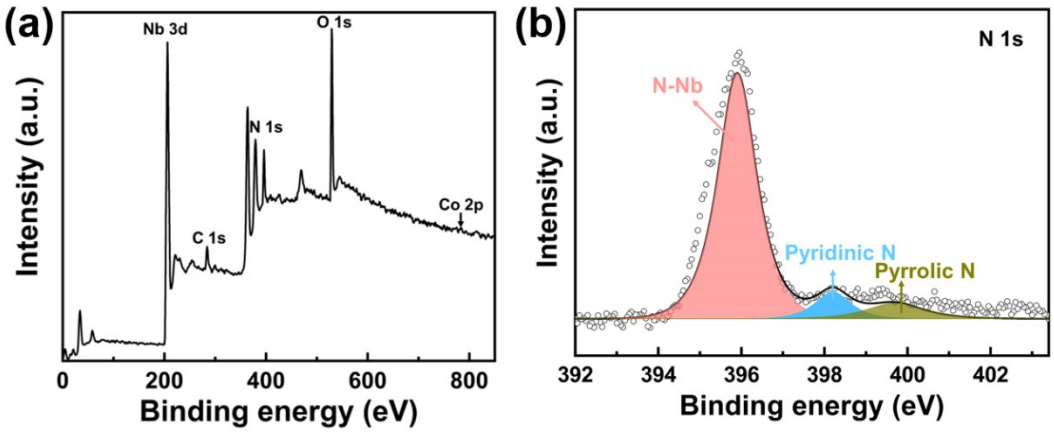

Fig. S5 (a) XPS survey spectrum of Co-NbN. (b) XPS fine N 1s spectrum of Co-NbN.

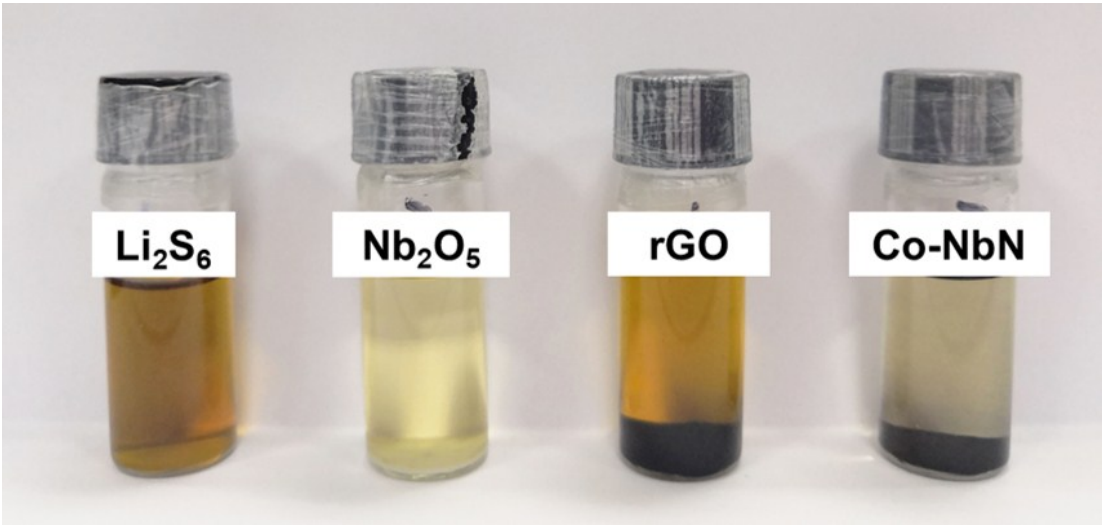

Fig. S6 A digital photograph of polysulfides adsorption test after adding Nb_2O_5, rGO and Co-NbN sample.

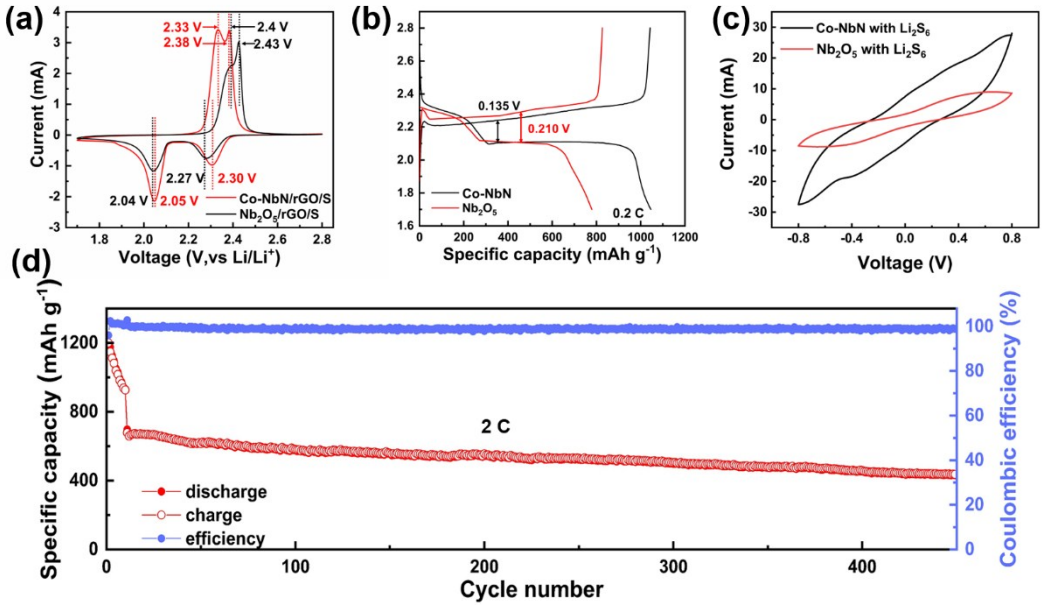

Fig. S7 (a) Cyclic voltammograms curves of Co-NbN/rGO/S and Nb_2O_5/rGO/S cathodes at the scan rate of 0.1 mV s^{-1}. (b) The typical galvanostatic charge-discharge voltage profiles of Co-NbN and Nb_2O_5 based cathodes at 0.2 C. (c) CV curves of symmetric batteries with Co-NbN and Nb_2O_5. (d) Long-term cycle performance of Co-NbN/rGO/S cathode at 2 C.

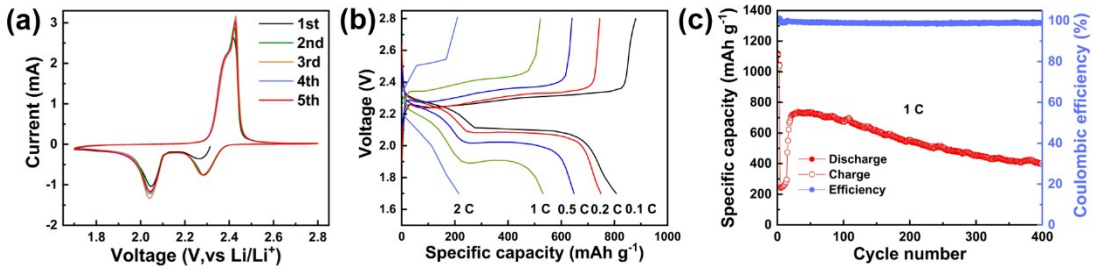

Fig. S8 The electrochemical performance of Nb_2O_5/rGO/S cathode. (a) CV curves at a scan rate of 0.1 mV s^{-1}. (b) The charge-discharge profiles at different current densities. (c) Long-term cycle performance at 1 C.

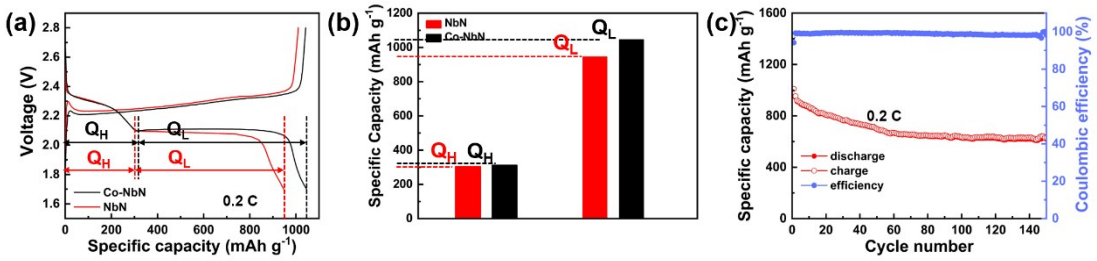

Fig. S9 (a) The CV curves of Li-S batteries with Co-NbN and NbN at 0.2 C (Q_H and Q_L represent the high and low discharge plateaus capacities, respectively). (b) The discharge capacities of Co-NbN/rGO/S and NbN/rGO/S cathode. (c) Long-term cycle performance of NbN/rGO/S cathode at 0.2 C.

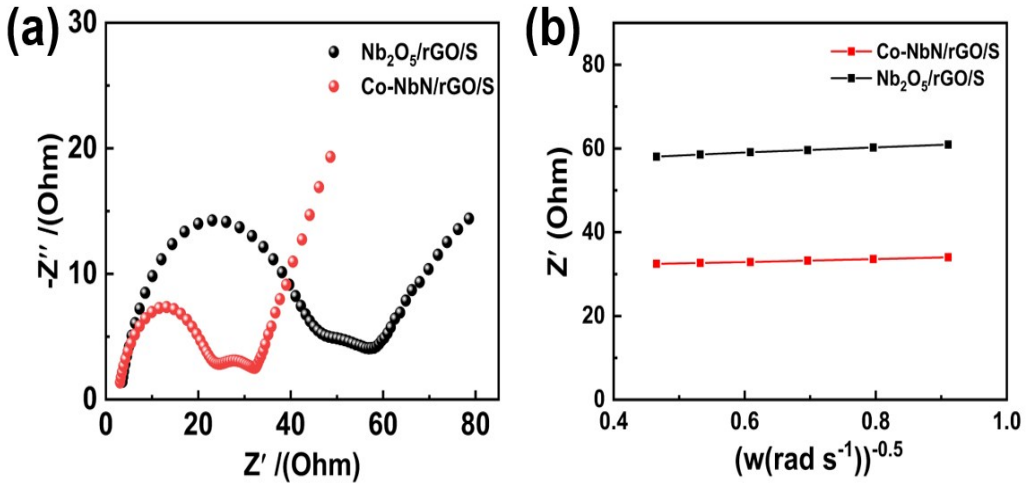

Fig. S10 (a) The electrochemical impedance spectra (EIS) of Co-NbN/rGO/S and Nb_2O_5/rGO/S cathode. (b) The relationship between the Z′ square root of angular frequency ($\omega^{-1/2}$).

To further elucidate excellent conductivity and electrochemical performance of cobalt doped NbN, electrochemical impedance spectra (EIS) was measured. The Warburg coefficient and Li^+ diffusion ability was calculated via following equations (1-2):

$$Zre = Re + Rct + \sigma\omega^{-0.5} \quad (1)$$

$$D_{Li^+} = 0.5(RT/AF^2C\sigma)^2 \quad (2)$$

Where R represents the gas constant, ω represents angular frequency, T represents the absolute temperature, A represents the electrode surface area, F represents the Faraday constant, C represents volume molar concentration of lithium ion and n is the charge transfer number.

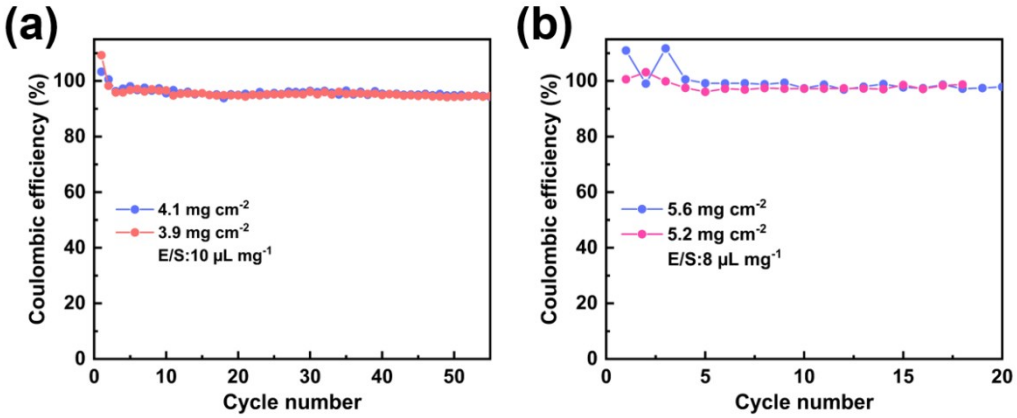

Fig. S11 Coulombic efficiency of Co-NbN/rGO/S cathode at different areal sulfur loading and the content of electrolyte.

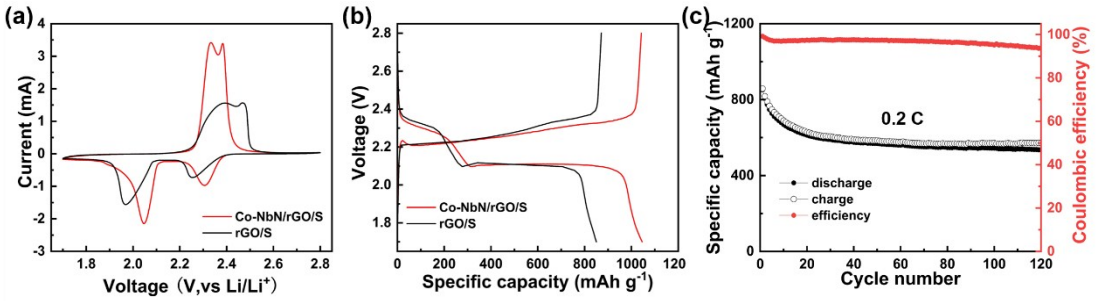

Fig. S12 Co-NbN/rGO/S and rGO/S cathodes (a) Cyclic voltammograms curves at the scan rate of 0.1 mV s-1 (b) Galvanostatic charge-discharge profiles at 0.2 C. (c) Cycle performance of rGO/S cathode at 0.2 C.

As shown in Fig. S12a, the CV curves of Co-NbN/rGO/S and rGO/S cathodes display that Co-NbN based cathode possesses two pairs of obvious redox peaks and lower oxidation potentials and higher reduction potentials, indicating that the electrochemical reversibility and polarization of Co-NbN based cathode are better than that of rGO based cathode. The typical galvanostatic charge-discharge profiles of Co-NbN/rGO/S and rGO/S are shown in Fig. S12b. The voltage gap of Co-NbN based cathode is smaller than that of rGO based cathode in charge-discharge profiles, which further suggests that Co-NbN can effectively reduce polarization of cathode. Co-NbN cathode has prolonged voltage plateaus, indicating that the rGO with weak physical adsorption ability is incapable of facilitating conversion of polysulfides. Fig. S12c exhibits the electrochemical performance of rGO/S cathode at 0.2 C. The rGO/S cathode displays rapid capacity fade and low coulombic efficiency, which indicates that rGO is incapable of efficiently inhibiting the shuttle effect and promoting the utilization of the sulfur.

Table S1. Comparison of the electrochemical performance of the porous cobalt doped NbN spheres and other similar materials reported in lithium-sulfur batteries. (1 C = 1675 mA g^{-1}).

Materials	Sulfur Content (%)	Areal mass of cathode (mg cm^{-2})	Current rate	Cycle number	Electrochemical performance (mAh g^{-1})	Reference
TiN	58.8	1.0	0.5 C	500	644	[1]
MoN-VN	58.5	1.13	1 C	500	555	[2]
TiN	70	1.3	1 C	400	560	[3]
C@TiN	71	1.1	1 C	150	741	[4]
WN	59	0.92	2 C	500	358	[5]
VN	70	1.6	1 C	800	368.6	[6]
Co/N-PCNs	68	0.8-1.0	1 C	200	633	[7]
g-C_3N_4/ graphene	65	1.1	100 mA g^{-1}	600	505	[8]
TiN	70	1.4-1.7	1 C	300	505.2	[9]
NbN		1.3	0.2 C	200	554.6	[10]
Cobalt doped NbN	72	1.2-1.7	1 C	800	404.5	This work
			2 C	450	431	
			0.2 C	150	706.5	

Reference

1. Z. Cui, C. Zu, W. Zhou, A. Manthiram and J. B. Goodenough, *Adv Mater*, 2016, **28**, 6926-6931.
2. C. Ye, Y. Jiao, H. Jin, A. D. Slattery, K. Davey, H. Wang and S. Z. Qiao, *Angew. Chem. Int. Ed.*, 2018, **57**, 16703-16707.
3. B. Qi, X. Zhao, S. Wang, K. Chen, Y. Wei, G. Chen, Y. Gao, D. Zhang, Z. Sun and F. Li, *J. Mater. Chem. A*, 2018, **6**, 14359-14366.
4. Y. Wang, R. Zhang, Y.-c. Pang, X. Chen, J. Lang, J. Xu, C. Xiao, H. Li, K. Xi and S. Ding, *Energy Storage Materials*, 2019, **16**, 228-235.
5. Z. D. Huang, Y. Fang, M. Yang, J. Yang, Y. Wang, Z. Wu, Q. Du, T. Masese, R. Liu, X. Yang, C. Qian, S. Jin and Y. Ma, *ACS Appl Mater Interfaces*, 2019, **11**, 20013-20021.
6. Y. Song, S. Zhao, Y. Chen, J. Cai, J. Li, Q. Yang, J. Sun and Z. Liu, *ACS Appl Mater Interfaces*, 2019, **11**, 5687-5694.
7. S. Liu, J. Li, X. Yan, Q. Su, Y. Lu, J. Qiu, Z. Wang, X. Lin, J. Huang, R. Liu, B. Zheng, L. Chen, R. Fu and D. Wu, *Adv Mater*, 2018, **30**, e1706895.
8. M. Wang, Q. Liang, J. Han, Y. Tao, D. Liu, C. Zhang, W. Lv and Q.-H. Yang, *Nano Res.*, 2018, **11**, 3480-3489.
9. C. Li, J. Shi, L. Zhu, Y. Zhao, J. Lu and L. Xu, *Nano Res.*, 2018, **11**, 4302-4312.
10. W. Qiu, C. An, Y. Yan, J. Xu, Z. Zhang, W. Guo, Z. Wang, Z. Zheng, Z. Wang, Q. Deng and J. Li, *J. Power Sources*, 2019, **423**, 98-105.